

Radiative and interfacial recombination in CdTe heterostructures

C. H. Swartz,^{1,a)} M. Edirisooriya,¹ E. G. LeBlanc,¹ O. C. Noriega,¹ P. A. R. D. Jayathilaka,¹ O. S. Ogedengbe,¹ B. L. Hancock,¹ M. Holtz,¹ T. H. Myers,¹ and K. N. Zaunbrecher²

¹Materials Science, Engineering, and Commercialization Program, Texas State University, 601 University Dr., San Marcos, Texas 78666, USA

²National Renewable Energy Laboratory, 15013 Denver West Parkway, Mississippi RSF200, Golden, Colorado 80401, USA

(Received 21 October 2014; accepted 16 November 2014; published online 2 December 2014)

Double heterostructures (DH) were produced consisting of a CdTe film between two wide band gap barriers of CdMgTe alloy. A combined method was developed to quantify radiative and non-radiative recombination rates by examining the dependence of photoluminescence (PL) on both excitation intensity and time. The measured PL characteristics, and the interface state density extracted by modeling, indicate that the radiative efficiency of CdMgTe/CdTe DHs is comparable to that of AlGaAs/GaAs DHs, with interface state densities in the low 10^{10} cm^{-2} and carrier lifetimes as long as 240 ns. The radiative recombination coefficient of CdTe is found to be near $10^{-10} \text{ cm}^3 \text{ s}^{-1}$. CdTe film growth on bulk CdTe substrates resulted in a homoepitaxial interface layer with a high non-radiative recombination rate. © 2014 AIP Publishing LLC.

[<http://dx.doi.org/10.1063/1.4902926>]

Cadmium telluride-based solar cells are now manufactured in large quantities as their conversion efficiency continues to improve. While short circuit currents have risen close to theoretical limits, the open circuit voltage continues to be hampered by the short lifetime of photocarriers in CdTe.¹ The rapid, non-radiative recombination of carriers in CdTe is largely attributed to surfaces and interfaces.² Wide band gap barriers of $\text{Cd}_{1-x}\text{Mg}_x\text{Te}$ alloy are known to be effective surface passivants for CdTe, greatly reducing non-radiative recombination.³ We produced heterostructures based on these two materials, to examine the passivation of parasitic surface and interface recombination and to better understand the rate of band-to-band radiative recombination in CdTe.

Given the electron and hole carrier concentrations n and p , the rate of radiative recombination is simply given by $B_{rad}np$. Reported values of the recombination parameter B_{rad} have ranged from $2\text{--}4 \times 10^{-9} \text{ cm}^{-3} \text{ s}^{-1}$.⁴⁻⁶ However, the Van Roosbroeck-Shockley (VRS) relationship between absorption and recombination⁷ yields a very different value: $B_{rad} = 1\text{--}2 \times 10^{-10} \text{ cm}^{-3} \text{ s}^{-1}$ when calculated from the absorption spectrum of CdTe.^{8,9} This discrepancy is worth further examination, because an understanding of both radiative and non-radiative recombination rates is essential for guidance in photovoltaic device design.

Photoluminescence intensity (PL-I) measurements are a standard tool for the monitoring of recombination-related energy levels and interface quality, without the need for contacts or electrically conducting substrates.¹⁰ Time-resolved photoluminescence (TRPL) decay measurements are often used for probing carrier lifetimes. We report a numerical method combining PL-I with TRPL which not only characterizes interface-related recombination but estimates the radiative recombination coefficient as well.

Structures were grown by molecular beam epitaxy (MBE) on InSb (100) and bulk CdTe (211)B substrates in a system described previously.¹¹ InSb substrates first had a $0.5 \mu\text{m}$ buffer layer of InSb grown by MBE in a III-Sb-specific chamber. Films consisted of 0.5 to $1.5 \mu\text{m}$ thick CdTe buffer layers on both substrates followed by double heterostructures (DH) consisting of a 500 to 1500 nm thick CdTe absorber layer between two 30 nm barriers of CdMgTe, capped by a 10 nm layer of CdTe to prevent potential oxidation of the Mg. Single heterostructures (SH) were also fabricated without the deeper CdMgTe barrier.

The excitation source for PL-I was an argon ion laser of 514 nm wavelength chopped at 400 Hz . A $6.5\times$ objective lens focused the laser light to give a $90 \mu\text{m}$ FWHM Gaussian spot on the sample. The absolute excitation power was varied with a series of calibrated neutral density filters and measured with a calibrated power meter. The luminescence was collected through the same objective, passed through optical filters to reject reflected laser light, and focused onto a Si photodiode. TRPL was measured by time-correlated single photon detection using a 640 nm fast pulse laser.

The band gap of the $\text{Mg}_x\text{Cd}_{1-x}\text{Te}$ barriers was measured by angle-dependent spectroscopic ellipsometry (SE). The barrier was modeled as a collection of Cody-Lorentz oscillators,¹² and the free parameters were fit to the ellipsometric data. The real and imaginary dielectric properties of the alloy barrier were extracted from this oscillator model, and the band gap was identified as a maximum in the real refractive index.¹³

Previous PL-I and TRPL modeling has commonly treated the minority carrier lifetime (τ) or the interfacial recombination velocity (S) as fixed material parameters.¹⁴⁻¹⁶ However, at all but the lowest excitation intensities, τ and S are not well-defined concepts.^{17,18} To properly characterize bulk and interfacial recombination, as in the DH illustrated in Figure 1, we have developed a rapid numerical algorithm to calculate the PL intensity, both in steady-state and as a

^{a)}E-mail: craig.swartz@txstate.edu. Tel. : (512) 245-1839. Fax: (512) 245-3675; Present address: RFM 3205, Texas State University, 601 University Drive, San Marcos, Texas 78666, USA

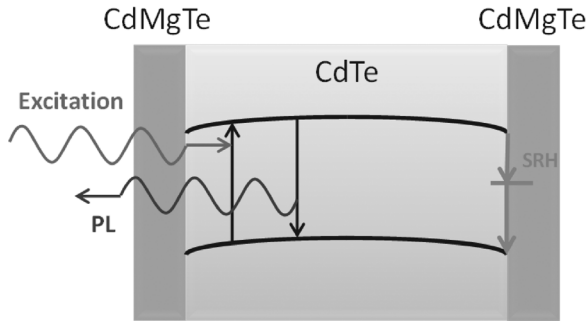


FIG. 1. Schematic of recombination in a CdMgTe/CdTe double heterostructure, consisting of an absorber layer between two barriers.

function of time. The model takes into account generation, recombination, diffusion, and drift, including the drift current effects resulting from the charging of recombination centers.¹⁹ Accordingly, the n -type carrier density is described by

$$\frac{dn}{dt} = -\mu_n V_{th} \frac{d^2 n}{dx^2} - \frac{d}{dx} (\mu_n n E) + I_0 \alpha e^{-\alpha x} + (B_{rad} + B_{SRH})(n_i^2 - np). \quad (1)$$

The p -type carrier density evolves in the same way, with the electron mobility μ_n replaced by the hole mobility, μ_p . Here, x is the depth, and I_0 and α are the intensity and absorption coefficient for the excitation light. B_{rad} and B_{SRH} determine the radiative and non-radiative recombination rates, and the term containing the intrinsic carrier concentration n_i accounts for thermal generation. The thermal voltage is $V_{th} = k_B T/q$, where $k_B T$ is the thermal energy. The fundamental charge is q , and E is the electric field derived from Poisson's equation

$$\frac{\epsilon dE}{q dx} = -n + p + N_D - N_A + Q_{SRH}, \quad (2)$$

where N_D and N_A are the donor and acceptor densities.

B_{SRH} and Q_{SRH} are the recombination coefficient and trapped charge due to Shockley-Read-Hall (SRH) centers. For reasons to be made clear below, they are assumed to be negligible except at the boundaries or interfaces, limited to a layer of small thickness Δx . As Auger recombination is believed to be negligible for CdTe,^{20,21} non-interfacial recombination is dominated by direct band-to-band radiative transitions.

SRH recombination is modeled, in steady state, by the standard expressions^{22,23}

$$B_{SRH} = \frac{N_T}{\Delta x} \left(\frac{n + n_1}{v_{thp} \sigma_p} + \frac{p + p_1}{v_{thn} \sigma_n} \right)^{-1}, \quad (3)$$

$$Q_{SRH} = \frac{N_T}{\Delta x} \left(\frac{v_{thp} \sigma_p p + v_{thn} \sigma_n n_1}{v_{thn} \sigma_n (n + n_1) + v_{thp} \sigma_p (p + p_1)} \right), \quad (4)$$

where $n_1 = N_C \exp[(E_T - E_G)/k_B T]$, $p_1 = N_V \exp[-E_T/k_B T]$, and N_C and N_V are the effective densities of states in the conduction and valence bands. N_T and E_T are the sheet density and energy of a recombination level, and other physical

TABLE I. The material parameters used in the numerical modeling, from Ref. 36. Capture cross sections taken from Ref. 37.

Parameter	Symbol	Value
Electron mobility	μ_n	800 cm ² /Vs
Hole mobility	μ_p	60 cm ² /Vs
Electron capture cross section	σ_n	10 ⁻¹² cm ²
Hole capture cross section	σ_p	10 ⁻¹⁵ cm ²
Conduction band effective mass	m_c^*	0.094 m_e
Valence band effective mass	m_v^*	0.81 m_e
Band gap	E_G	1.48 eV
Permittivity	ϵ	10.4 ϵ_0

parameters used are listed in Table I. Thermal velocities and effective state densities were determined from the conduction and valence band effective masses m_c^* and m_v^* . The predicted PL signal intensity is the integral of $B_{rad} np$ over x , and the trap properties N_T and E_T are varied to achieve a least squares fit to the PL-I data. Further details of the rapid modeling algorithm have been published elsewhere.²⁴

To take into account time-resolved decay behavior, the simulated intensity I_0 was replaced with a time dependent $I_0(t)$ which matched the Gaussian laser pulse. Furthermore, the standard SRH expressions (3) and (4) were not used, as they were originally derived only for the steady state limit.²⁵ The standard expressions are usually applied when analyzing time-resolved measurements, such as intensity-dependent photoconductivity decay.²⁶ However, this is not valid after a photo-excitation, unless the trap occupation ratio happens to be the same under both dark and illuminated conditions. This is not likely unless the excitation is limited to very low intensities. Instead, the capture rates ($n \sigma_n N_T^u v_{thn}$) and spontaneous emission rates ($n_1 \sigma_n N_T^o v_{thn}$) were individually calculated at each time step, for holes as well as electrons. Here, the superscripts o and u refer to the concentration of occupied and unoccupied traps.

For the samples with PL data reported here, the band gap of the Cd_{1-x}Mg_xTe barriers was determined to be 2.1 ± 0.1 eV using SE. According to a composition-band gap relationship²⁷ determined using energy dispersive spectroscopy of thick samples coupled with cathodoluminescence measurements, this corresponds to a composition of $x = 0.35 \pm 0.02$. An atom probe tomography (APT) measurement carried out on a sample with a SE-determined composition of $x = 0.37$ was found to be in good agreement, with the APT measurement yielding $x = 0.376$.

The normalized PL efficiency (the PL signal divided by the excitation intensity) as a function of excitation is shown in Figure 2 for various structures. Note that increasing the photo-injection, and hence increasing the carrier concentrations n and p , should cause the SRH recombination rate to increase in an ultimately linear fashion, while the radiative rate should increase quadratically. Thus, the quantum efficiency for radiative recombination (at least the internal quantum efficiency) will tend to approach 100% at higher intensities, and the normalized PL—being divided by the excitation intensity—should reflect this leveling off.

Bare CdTe samples uniformly exhibited very low PL efficiency at any excitation intensity, regardless of any

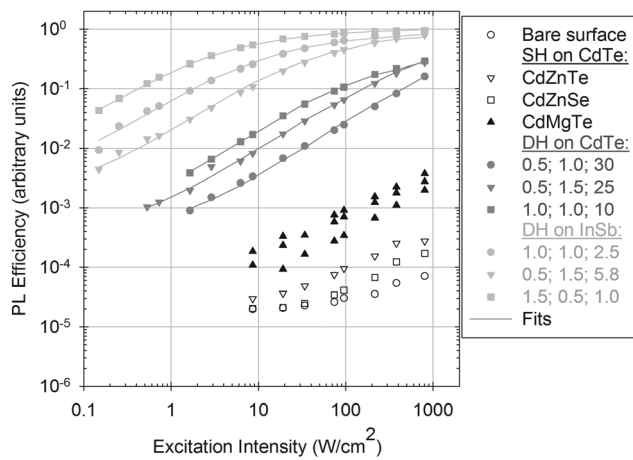


FIG. 2. The normalized PL dependence on excitation intensity shows the effect of single sided barriers (SH), two sided CdMgTe barriers (DH) on CdTe substrates, and DH growth on InSb substrates. The buffer layer thickness (μm), the absorber layer thickness (μm), and the resulting trap density (10^{10} cm^{-2}) are indicated for each DH. The measured PL signal was divided by the excitation intensity to obtain efficiency.

differences in crystalline quality, dislocation density, or growth technique. SHs were attempted using CdZnTe and CdZnSe as top surface barriers on CdTe, but with little improvement. CdMgTe SHs exhibited more than an order of magnitude improvement, an increase consistent with the material's larger type I band offset with both strong electron and hole confinement.²⁸

More surprisingly, the use of a DH granted an additional two orders of magnitude improvement. While the lack of a confining bottom barrier might allow some photocarriers to leave the light collection area, the large spot size and the low absorption index for near-band gap PL output would limit this to a small effect. Therefore, the homoepitaxial interface between the CdTe buffer layer and the bulk CdTe is likely a major source of recombination.

Fig. 2 shows the PL-I efficiency of the DHs with thickness and N_T . The trap energy E_T was in all cases $100 \pm 25 \text{ meV}$ above the valence band. This is consistent with the disorder-induced gap state (DIGS) model of interfacial recombination, which has been demonstrated to consistently explain PL-I and capacitance-voltage (C-V) results in other compound semiconductors.^{29,30} The DIGS model suggests that a material such as CdTe with a charge neutrality level high in the band gap at 1.12 eV (Ref. 31) would be dominated by (donor-like) recombination centers low in the gap. The fact that the PL-I of a DH tends to increase with absorber layer thickness suggests that interfacial recombination continues to be the primary non-radiative recombination pathway with these barriers. Increasing the thickness from 1.0 to $1.5 \mu\text{m}$ strengthens the PL-I, even as the extracted interfacial trap density N_T remains nearly unchanged.

However, increase in the buffer layer thickness appears to have even more impact on PL intensity, surpassing absorber layer thickness as the major factor. This occurs because thicker buffer layers are found to reduce interfacial trap density. When the buffer layer's thickness was increased from 0.2 to $1.0 \mu\text{m}$, the PL-I efficiency for a $1.0 \mu\text{m}$ thick absorber improved by a factor of five, without any change to the absorber layer thickness, by decreasing the interfacial

trap density to $N_T = 1 \times 10^{11} \text{ cm}^{-2}$. This indicates that the parasitic homoepitaxial interfacial layer deduced from the SH results may have some residual influence on the bottom barrier, either from impurity interdiffusion or deviation from flat band, requiring a thicker layer of MBE-CdTe to minimize the effect.

As an alternative to possible surface preparation issues with bulk CdTe, (100) InSb substrates were employed. For a $1.0 \mu\text{m}$ thick absorber DH on a $1.0 \mu\text{m}$ thick CdTe buffer, growth on an InSb substrate markedly decreased the number of dislocations visible by confocal microscopy. This was accompanied by a factor of 5 increase in the PL-I from similar structures grown on a bulk CdTe substrate. These samples had uniformly low defect concentration without dark line defects unlike some other similar structures grown on InSb(100) reported in the literature.³²

As with the CdTe substrates, a thicker $1.5 \mu\text{m}$ absorber layer was tested on InSb substrates. However, the use of InSb limits the total DH thickness plus buffer layer thickness to about $2 \mu\text{m}$ due to the onset of misfit dislocations as the thickness approaches the critical thickness of CdTe, which is nearly but not fully lattice matched to InSb.³³ Thus, a $1.5 \mu\text{m}$ absorber layer necessitated a $0.5 \mu\text{m}$ buffer. The thinner buffer resulted in a lower PL-I, again suggesting an interaction with the substrate/epilayer interface.

When the buffer instead was grown $1.5 \mu\text{m}$ thick with a $0.5 \mu\text{m}$ absorber layer, the PL-I increased to the maximum intensity so far observed in any CdTe-based structure, with a trap density of $1 \times 10^{10} \text{ cm}^{-2}$, comparable to the highest quality AlGaAs-GaAs DHs. Indeed, the measured luminescence intensity at $>100 \text{ Wcm}^{-2}$ from the CdTe DH was a factor of 5.4 larger than that measured for reference AlGaAs-GaAs DHs used as standards, which had been previously characterized to give nearly 100% internal efficiency.^{14,34} Calculation of the different reflection losses³⁵ and laser absorption differences between the two structures indicates an expected PL enhancement of 5.5 for the CdTe DH, very close to what was measured.

Films with the highest PL intensity tend to have the longest TRPL lifetime, as would be expected from a reduction in the amount of non-radiative recombination. At all but the lowest injection levels, the TRPL signal decay is generally non-exponential in nature. This is partly because of transport time, as the initial pulse diffuses throughout the thickness of the sample, and partly because of the excitation dependence of the recombination rate; that is, the same phenomenon measured by PL-I. The TRPL trace of the DH having a $1\text{-}\mu\text{m}$ buffer and $1 \mu\text{m}$ absorber grown on an InSb substrate is shown in Figure 3. This can be simulated using only the physical parameters in Table I and the value of N_T extracted from the PL-I. Given that there are *no free parameters* in the model, the agreement is quite good. A key requirement is the use of the VRS-predicted value of $B_{rad} = 1 \times 10^{-10} \text{ cm}^3 \text{ s}^{-1}$. Larger estimations of B_{rad} appearing in the literature are contradicted by these results, as the higher trap density needed to then account for the PL-I requires a decay significantly faster than the observed TRPL lifetimes.

$\text{Mg}_{1-x}\text{Cd}_x\text{Te}$ barriers with composition $x \sim 0.35$ are very effective at reducing recombination at the surfaces and interfaces of CdTe. The use of double heterostructures

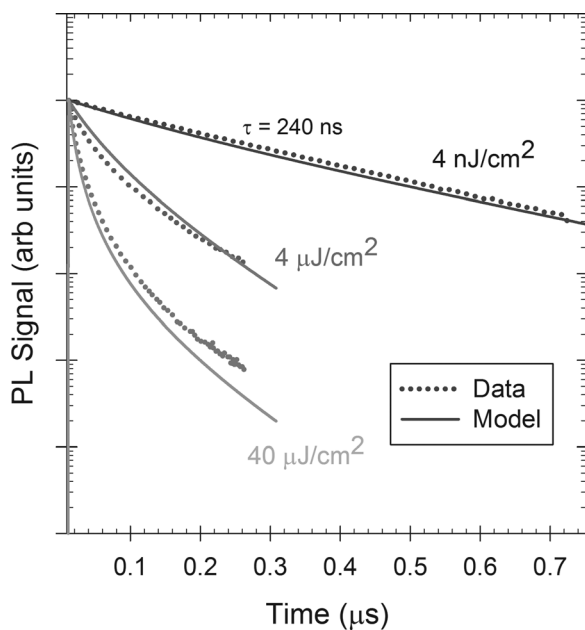


FIG. 3. The trap parameters resulting from the fit to the PL-I data ($N_T = 2.5 \times 10^{10} \text{ cm}^{-2}$) were used to simulate the time dependent distribution of carriers after a pulse of photo-generated electron-hole pairs—without the use of any additional parameters. The simulated PL intensity yields a decay consistent with the experimental TRPL lifetimes measured on the same sample. In this case, TRPL was performed with several different pulse intensities. We note that the low injection lifetime is one of the longest ever measured for CdTe.

resulted in high PL efficiency for CdTe, comparable to that observed for AlGaAs/GaAs DH. A numerical model was used to analyze both the PL-I and TRPL characteristics in combination. The simulation quantitatively reveals interfacial trap densities as low as $N_T = 1 \times 10^{10} \text{ cm}^{-2}$, and suggests that the radiative recombination coefficient of CdTe is $B_{rad} = 1 \times 10^{-10} \text{ cm}^3 \text{ s}^{-1}$.

Funding from the Alliance for Sustainable Energy, LLC, the manager and operator of the National Renewable Energy Laboratory for the U.S. Department of Energy through Contract No. DEAC36-08GO28308 FPACE II: Approaching the S-Q Limit with Epitaxial CdTe, Subcontract Z EJ-4-42007-0 is acknowledged. We would like to thank B. Gorman for APT results, and NREL for SIMS.

¹M. Gloeckler and J. R. Sites, *Thin Solid Films* **480**, 241 (2005).

²J. R. Sites and J. Pan, *Thin Solid Films* **515**, 6099 (2007).

³M. J. DiNezza, X.-H. Zhao, S. Liu, A. P. Kirk, and Y.-H. Zhang, *Appl. Phys. Lett.* **103**, 193901 (2013).

- ⁴R. Cohen, V. Lyahovitskaya, E. Poles, A. Liu, and Y. Rosenwaks, *Appl. Phys. Lett.* **73**, 1400 (1998).
- ⁵R. K. Ahrenkiel, B. M. Keyes, D. L. Levi, K. Emery, T. L. Chu, and S. S. Chu, *Appl. Phys. Lett.* **64**, 2879 (1994).
- ⁶X.-H. Zhao, M. J. DiNezza, S. Liu, S. Lin, Y.-H. Zhang, and Y. Zhao, *J. Vac. Sci. Technol. B* **32**, 040601 (2014).
- ⁷W. van Roosbroeck and W. Shockley, *Phys. Rev.* **94**, 1558 (1954).
- ⁸A. P. Kirk, M. J. DiNezza, S. Liu, X.-H. Zhao, and Y.-H. Zhang in *39th Photovoltaic Specialists Conference (PVSC) Tampa Bay, FL 2013* (IEEE, 2013), p. 2515.
- ⁹A. E. Rakhshani, *J. Appl. Phys.* **81**, 7988 (1997).
- ¹⁰M. Passlack, R. N. Legge, D. Convey, Z. Yu, and J. K. Abrokwh, *IEEE Trans. Instrum. Meas.* **47**, 1362 (1998).
- ¹¹J. Chai, K.-K. Lee, K. Doyle, J. H. Dinan, and T. H. Myers, *J. Electron. Mater.* **41**, 2738 (2012).
- ¹²J. Price, P. Y. Hung, T. Rhoad, B. Foran, and A. C. Diebold, *Appl. Phys. Lett.* **85**, 1701 (2004).
- ¹³D. Poelman and J. Vennik, *J. Phys. D: Appl. Phys.* **21**, 1004 (1988).
- ¹⁴M. Passlack, M. Hong, J. P. Mannaerts, J. R. Kwo, and L. W. Tub, *Appl. Phys. Lett.* **68**, 3605 (1996).
- ¹⁵A. A. Demkov and A. Navrotsky, *Materials Fundamentals of Gate Dielectrics* (Springer, Dordrecht, The Netherlands, 2005), p. 403ff.
- ¹⁶J. A. Giesecke, R. A. Sinton, M. C. Schubert, S. Riepe, and W. Warta, *IEEE J. Photovoltaics* **3**, 1311 (2013).
- ¹⁷P. De Visschere, *Solid-State Electron.* **29**, 1161 (1986).
- ¹⁸B. Adamowicz and H. Hasegawa, *Jpn. J. Appl. Phys.* **37**, 1631 (1998).
- ¹⁹A. G. Aberle, S. Glunz, and W. Warta, *J. Appl. Phys.* **71**, 4422 (1992).
- ²⁰A. Haug, *J. Phys. C: Solid State Phys.* **16**, 4159 (1983).
- ²¹J. Vaitkus, R. Tomašūnas, J. Kutra, M. Petrauskas, R. Rimkūnas, and A. Žindulis, *J. Cryst. Growth* **101**, 826 (1990).
- ²²S. M. Sze, *Physics of Semiconductor Devices* (Wiley, New York, 1982), p. 85.
- ²³J. Kubat, H. Elhadidy, J. Franc, R. Grill, E. Belas, P. Hoschl, and P. Praus, *IEEE Trans. Nuc. Sci.* **56**, 1706 (2009).
- ²⁴C. H. Swartz, O. C. Noriega, P. A. R. D. Jayathilaka, M. Edirisooriya, X.-H. Zhao, M. J. DiNezza, S. Liu, Y.-H. Zhang, and T. H. Myers, *40th Photovoltaic Specialists Conference (PVSC), Denver, CO* (IEEE, 2014), p. 2419.
- ²⁵W. Shockley and W. T. Read, *Phys. Rev.* **87**, 835 (1952).
- ²⁶S. Rein, T. Rehrl, W. Warta, and S. W. Glunz, *J. Appl. Phys.* **91**, 2059 (2002).
- ²⁷A. Waag, H. Heinke, S. Scholl, C. R. Becker, and G. Landwehr, *J. Cryst. Growth* **131**, 607 (1993).
- ²⁸S. Abdi-Ben Nasrallah, S. Mnasri, N. Sfina, N. Bouarissa, and M. Said, *J. Alloys Compd.* **509**, 7677 (2011).
- ²⁹H. Hasegawa and T. Sawada, *Thin Solid Films* **103**, 119 (1983).
- ³⁰H. Hasegawa and M. Akazawa, *Appl. Surf. Sci.* **254**, 8005 (2008).
- ³¹W. Mönch, *Appl. Phys. A* **87**, 359 (2007).
- ³²K. Alberi, B. Fluegel, M. J. DiNezza, S. Liu, Y. Zhang, and A. Mascarenhas, *Appl. Phys. Express* **7**, 065503 (2014).
- ³³C. Fontaine, J. P. Gailliard, S. Magli, A. Million, and J. Piagnet, *Appl. Phys. Lett.* **50**, 903 (1987).
- ³⁴J.-B. Wang, D. Ding, S. R. Johnson, S.-Q. Yu, and Y.-H. Zhang, *Phys. Status Solidi B* **244**, 2740 (2007).
- ³⁵V. Zwiller and G. Björk, *J. Appl. Phys.* **92**, 660 (2002).
- ³⁶O. Madelung, *Semiconductors: Data Handbook*, 3rd ed. (Springer-Verlag, Heidelberg, Germany, 2004), p. 232ff.
- ³⁷M. Gloeckler, A. L. Fahrenbruch, and J. R. Sites, *3rd World Conference on Photovoltaic Energy Conversion Osaka, Japan* (IEEE, 2003), p. 491.